Asian Journal of Chemistry; Vol. 37, No. 12 (2025), 3102-3110
ASIAN JOURNAL OF CHEMISTRY
https://doi.org/10.14233/ajchem.2025.34750

Design, Synthesis, Characterization and Molecular Docking Studies of Some Pyrrolotriazine containing 1*H*-Pyrazole Derivatives as Anticancer Agent Against Breast Cancer

DISHA M. DHABARDE*, JAGDISH R. BAHETI and RUPAL K. DESHMUKH

Department of Pharmaceutical Chemistry, Kamla Nehru College of Pharmacy, Butibori, Nagpur-441108, India

*Corresponding author: E-mail: dishamandave30@gmail.com

Received: 22 August 2025 *Accepted*: 19 October 2025 *Published online*: 30 November 2025 AJC-22201

Pyrrolotriazine containing 1(*H*)pyrazole and its derivatives were designed, synthesized and screened for anticancer activity. Novel pyrazole derivatives incorporating a pyrrolotriazine moiety were rationally designed and synthesized *via* the Claisen-Schmidt condensation pathway. Initially, pyrrolotriazine was obtained through the condensation of pyrrole-2-carbaldehyde with hydroxylamine. Subsequent acetylation with acetyl chloride yielded acetylpyrrolotriazine, which was then condensed with various substituted benzaldehydes to afford pyrrolotriazine-based chalcones. These chalcone intermediates, upon cyclization with hydrazine hydrate, produced the target pyrazole-containing pyrrolotriazine derivatives. The synthesized compounds were characterized by spectroscopic techniques and evaluated for their potential anticancer activity against breast cancer cell lines. Docking study of synthesized compounds (**R1-15**) were performed by using PDB ID 8DUG with docking score of -10.5 Kcal/mol. Among the designed compounds, pyrazole derivatives (**R1-15**) exhibiting the highest binding affinities were synthesized and characterized using various spectroscopic techniques. Anticancer activity of synthesized compounds was evaluated against the human breast cancer cell line MCF-7, compounds **R1**, **R2** and **R13** showed significant cytotoxic activity. Among this 4-fluoro substituent possess highest anti-breast cancer activity due to lipohilicity, membrane permeability and balance between electronic and steric effect, hence suggested that the synthesized compounds would be useful as anticancer drugs.

Keywords: Anticancer activity, Binding affinity, Claisen Schmidt condensation, MTT assay, Pyrazole, Pyrrolotriazine.

INTRODUCTION

Heterocyclic compounds containing heteroatoms such as sulfur, nitrogen and oxygen particularly those incorporating structural motifs like thiophenes, pyrazoles and imines continue to attract significant attention from medicinal chemists and researchers due to their diverse biological and pharmacological activities [1,2]. Fused heterocycles, containing interconnected rings with heteroatoms, are key scaffolds in anticancer drug discovery due to their structural rigidity, target specificity, and versatile chemical modifiability, as reflected in several clinically approved agents [3-7]. Fused heterocycles are also of high interest in designing drugs targeting kinases due to their ability to provide selectivity for a specific kinase or its isoform [8-10].

Cancer, an abysmal disease, characterized by the uncontrolled division and proliferation of cells. Despite having a challenging prognosis, it nevertheless has a significant death rate due to the disease itself and the effects of treatment, as well as an extremely vigorous treatment regimen [11,12]. According to the World Health Organization (WHO), cancer accounted for approximately 9.6 million deaths globally in 2018 [13]. Among pediatric and adolescent populations, leukemia represents the most common form of cancer, contributing to nearly one-third of all diagnosed cases [14]. According to a research, there would be 29.50 million new cases of cancer per year and 16.40 million fatalities from the disease by 2024 [15].

For the treatment of cancer, various approaches have been developed. Both chemotherapy, radiotherapy and immunotherapy have a number of side effects that reduce the effectiveness of drugs and can reduce the quality of life of patients [16,17]. Therefore, it is extremely important to search for new therapeutic strategies to develop drugs with a better pharmacological profile that act specifically on cancer cells and minimize toxic effects on normal cells. With 25% of cases, breast cancer is the most prevalent kind in women. for this

kind of tumor, the chemotherapeutic option uses monoclonal antibodies like trastuzumab to target specific areas [18]. Since, it can block the estrogen receptors α and β, new molecules derived from hybrid heterocyclic compounds showed promising results against breast tumors by stopping the growth of aberrant cells. The anticancer potential of pyrrolotriazine-containing 1*H*-pyrazole derivatives has been extensively explored in recent years due to the persistent challenges in treating multidrug-resistant tumors with conventional therapies and the high toxicity associated with combination chemotherapy regimens [19].

In present study, novel fifteen pyrrolotriazine-containing 1*H*-pyrazole derivatives were synthesized and evaluated for their anticancer potential against MCF-7 breast cancer cell lines. Furthermore, molecular docking studies were conducted using PDB ID: 8DUG to investigate the binding interactions and identify the key active site residues involved in ligand-protein recognition.

EXPERIMENTAL

Chemicals and solvents used were of laboratory grade and procured from different reputed commercial chemical suppliers. Open capillary method was used to determine the melting points and the values are uncorrected. To monitor the progress of the reactions acetonitrile and benzene (3:1) were used as solvent systems. The developed TLC plates were visualized by exposing them to iodine vapours. The ultraviolet (UV) spectra were recorded using a Shimadzu UV-visible spectrophotometer model 1800 using HPLC-grade ethanol as solvent. The infrared (IR) spectra compounds were recorded on a IRSpirit FTIR spectrophotometer using the KBr pellet technique in the 4000-400 cm^{-1} range. The ^{1}H NMR and ^{13}C NMR spectra were recorded in methanol using NMR Bruker Advance NEO 500 MHz spectrometer. Mass spectra were recorded on an electron impact mass spectrometer at 70 eV ionizing beam and using a direct insertion probe.

Synthesis of pyrrolotriazine-containing 1*H*-pyrazole derivatives (R1-15): The synthesis of novel pyrrolotriazine-containing 1*H*-pyrazole derivatives (**R1–R15**) was carried out *via* a multi-step reaction sequences.

Synthesis of 1*H*-pyrrole-2-carbonitrile (Step-1): A mixture containing 1*H*-pyrrole-2-carbaldehyde (1 g) and hydroxylamine hydrochloride (2 g) were thoroughly mixed and then subjected to microwave irradiation at a power of 300 W for 2 min using a laboratory microwave oven followed by the addition of 2 mL dichloromethane, while stirring the mixture. The filtrate was collected and the solvent was evaporated to obtain the crude product, which was dried over anhydrous sodium sulphate. The product was recrystallized by methanol which was further purified by column chromatography.

Synthesis of pyrrolo[2,1-*f*][1,2,4]triazin-4-amine (Step-2): In round bottom flask, pyrrole-2-carbonitrile (1 g) and chloroamine (0.85 g) was added. The mixture was dissolved in 5 mL of methanol and subjected to microwave irradiation at 300 W for 2 min. To the cyclized reaction mixture, 0.72 g formamidine and 2 mL of methanol were added. The mixture was again irradiated under microwave conditions at 300 W for 2 min. Upon completion of the reaction, the crude product was collected by filtration and dried at room temperature. The solid was then purified by recrystallized by methanol to obtain the compound.

Synthesis of 1-(4-aminopyrrolo[2,1-*f*][1,2,4]-triazin-6-yl)ethan-1-one (Step-3): In a round bottom flask, 0.245 g of pyrrolo[2,1-*f*][1,2,4]triazin-4-amine was added to 10 mL of DMF. The mixture was stirred thoroughly until complete dissolution was achieved followed by the addition of 2 mL acetyl chloride. The flask was placed in a microwave oven and irradiated at 300 W for 3 min. The reaction mixture was cooled to room temperature. Then 2 mL of water was added to the reaction mixture and stirred to quench excess acetyl chloride. The mixture was transferred to a separatory funnel and extracted with ethyl acetate (2 × 5 mL). The combined organic layers were dried over anhydrous sodium sulphate. The drying agent was removed by filtration which was further purified by column chromatography.

(2*E*)-1-(4-amino-1,4-dihydropyrrolo[2,1-*f*][1,2,4]triazin-6-yl)-3-phenylprop-2-en-1-one (Step-4:): In a round bottom flask, substituted aldehyde (0.001 mol) was mixed with 1-(4-aminopyrrolo[2,1-*f*][1,2,4]triazin-6-yl)ethanone (0.001 mol) and dissolved in 3 mL of ethanol. To this mixture, aqueous KOH (0.003 mol) was added slowly. The reaction mixture was then placed in a microwave oven set at 180 W and heated for 2-3 min under microwave irradiation. Upon completion of the reaction, the mixture was allowed to cool to room temperature. The resulting solid product was collected by filtration, washed with cold ethanol and dried. The crude product was further purified by recrystallization by using methanol.

Synthesis of 6-[5-(4-substituted phenyl)-4,5-dihydro-1*H*-pyrazol-3-yl]pyrrolo[2,1-*f*][1,2,4]triazin-4-amine (Step-5): A quantity of 1 g of synthesized chalcone as obtained from step 4 was combined with 1 mL of acetic acid, followed by the careful addition of 3 mL of hydrazine hydrate. Subsequently, 3 mL of ethanol were added to the mixture and then the complete solution was then subjected to microwave irradiation at a power of 300 W for a duration of 2 min. Upon completion of the heating process, the round bottom flask was allowed to cool to room temperature. The precipitated solid was collected, recrystallized from methanol and then purified by column chromatography.

6-[5-[(2-Hydroxyphenyl)]-4,5-dihydro-1*H*-pyrazol-3-yl] pyrrolo[2,1-*f*][1,2,4]triazin-4-amine (R1): Yield: 87%; colour: brown; m.w.: 296.33; m.p.: 202-204 ºC; R_f: 0.75 (benzene and acetonitrile); λ_{max}: 293.60; IR (KBr, ν_{max}, cm^{-1}): 3686.76 (-OH), 3200.42 (NH_2), 1658.68 (C=N), 1608.77, 1486.11 (C=C); ^{1}H NMR (500 MHz, $CDCl_3$) δ ppm: 9.06 (NH), 8.59 (OH), 7.29-8.20 (m, ArH), 6.92 (NH_2), 3.92 (CH_2); ^{13}C NMR (500 MHz, $CDCl_3$) δ ppm: 76.17, 77.91, 77.23, 117.71, 132.57, 133.49, 147.71, 153.31; MS: (*m/z*): Calcd. for $C_{15}H_{16}N_6O$ (296.3312); Found: 297.0501.

6-[5-[(4-Nitrophenyl)]-4,5-dihydro-1*H*-pyrazol-3-yl]-pyrrolo[2,1-*f*][1,2,4]triazin-4-amine (R2): Yield: 95%; colour: black; m.w.: 323.40; m.p.: 198-200 ºC; R_f: 0.78 (benzene and acetonitrile); λ_{max}: 265.60; IR (KBr, ν_{max}, cm^{-1}): 3187.58 (-NH_2), 3089 (C-H); 1658.68 (C=N), 1608.77, 1486.11 (C=C), 1558.85, 1333.51 (-NO_2); ^{1}H NMR (500 MHz, $CDCl_3$) δ ppm: 8.56 (NH), 7.23-7.85 (m, Ar-H), 6.02 (NH_2), 2.09 (CH_2); ^{13}C NMR (500 MHz, $CDCl_3$) δ ppm: 76.78, 77.04, 77.29, 114.31, 120.06,

126.64, 128.95, 129.10, 129.43, 138.22, 139.07, 143.62, 148.19; MS: (*m/z*): Calcd. for $C_{15}H_{15}N_7O_2$ (323.3094); Found: 324.9760.

6-[5-[4-(3-Hydroxyphenyl)]-4,5-dihydro-1*H*-pyrazol-3-yl]pyrrolo[2,1-*f*][1,2,4]triazin-4-amine (R3): Yield: 82%; colour: yellow; m.w.: 341.32; m.p.: 210-212 ºC; R_f: 0.89 (benzene and acetonitrile); λ_{max}: 204.80; IR (KBr, ν_{max}, cm^{-1}): 3616.87 (-OH), 3264.60 (-NH_2), 3154.78 (C-H), 1687.21 (C=N), 1597.36, 1459.01 (C=C).

6-[5-[4-(4-Chlorophenyl)]-4,5-dihydro-1*H*-pyrazol-3-yl]pyrrolo[2,1-*f*][1,2,4]triazin-4-amine (R4): Yield: 80.43%; colour: brown; m.w.: 296.33; m.p.: 212-214 ºC; R_f: 0.75 (benzene and acetonitrile); λ_{max}: 306.80; IR (KBr, ν_{max}, cm^{-1}): 3264.60 (-NH_2), 1627.31 (C=N), 1383.43 (C=C), 547.64 (-Cl),

6-[5-[4-(4-Bromophenyl)]-4,5-dihydro-1*H*-pyrazol-3-yl]pyrrolo[2,1-*f*][1,2,4]triazin-4-amine (R5): Yield: 76%; colour: brownish; m.w.: 330.77; m.p.: 204-206 ºC; R_f: 0.76 (benzene and acetonitrile); λ_{max}: 357.00; IR (KBr, ν_{max}, cm^{-1}): 3338.76 (-NH_2), 3171.89 (C-H), 1687.21 (C=N), 1620.18, 1406.24 (C=C), 557.65 (-Br).

6-[5-[(4-Methoxyphenyl)]-4,5-dihydro-1*H*-pyrazol-3-yl]pyrrolo[2,1-*f*][1,2,4]triazin-4-amine (R6): Yield: 76%; colour: light brown; m.w.: 323.40; m.p.: 208-210 ºC; R_f: 0.62 (benzene and acetonitrile); λ_{max}: 306.20; IR (KBr, ν_{max}, cm^{-1}): 3616.11 (-OH), 3216.11 (-NH_2), 3074.91 (C-H), 1687.21 (C=N), 1621.66, 1463.29 (C=C), 1263.62 (C-O).

6-[5-[Phenyl)]-4,5-dihydro-1*H*-pyrazol-3-yl]pyrrolo-[2,1-*f*][1,2,4]triazin-4-amine (R7): Yield: 75%; colour: yellow; m.w.: 359.22; m.p.: 184-186 ºC; R_f: 0.74 (benzene and acetonitrile); λ_{max}: 300.20; IR (KBr, ν_{max}, cm^{-1}): 3194.71 (-NH_2), 3023.57 (C-H), 1682.93 (C=N), 1604.49, 1493.24 (C=C),

6-[5-[(4-Hydroxyphenyl)]-4,5-dihydro-1*H*-pyrazol-3-yl]pyrrolo[2,1-*f*][1,2,4]triazin-4-amine (R8): Yield: 72%; colour: yellow; m.w.: 310.35; m.p.: 210-212 ºC; R_f: 0.56 (benzene and acetonitrile); λ_{max}: 290.40; IR (KBr, ν_{max}, cm^{-1}): 3618.30 (-OH), 3049.24 (C-H), 3171.89 (-NH_2), 1647.26 (C=N), 1457.59 (C=C),

6-[5-[(2-Methylphenyl)]-4,5-dihydro-1*H*-pyrazol-3-yl]-pyrrolo[2,1-*f*][1,2,4]triazin-4-amine (R9): Yield: 91%; colour: yellow; m.w.: 280.33; m.p.: 174-176 ºC; R_f: 0.56 (benzene and acetonitrile); λ_{max}: 208.00; IR (KBr, ν_{max}, cm^{-1}): 3304.53 (-NH_2), 3099.16 (C-H), 1553.18 (C=N), 1400.54 (C=C), 1357.54 (-CH_3).

6-[5-[(3-Bromophenyl)]-4,5-dihydro-1*H*-pyrazol-3-yl]-pyrrolo[2,1-*f*][1,2,4]triazin-4-amine (R10): Yield: 77%; colour: grey; m.w.: 296.33; m.p.: 186-188 ºC; R_f: 0.78 (benzene and acetonitrile); λ_{max}: 297.20; IR (KBr, ν_{max}, cm^{-1}): 3206.12 (-NH_2), 3070.63 (C-H), 1664.39 (C=N), 1608.77, 1407.64 (C=C), 1400.54 (-CH_3), 496.32 (-Br),

6-[5-[(3-Nitrophenyl)]-4,5-dihydro-1*H*-pyrazol-3-yl]-pyrrolo[2,1-*f*][1,2,4]triazin-4-amine (R11): Yield: 89%; colour: black; m.w.: 294.35; m.p.: 210-212 ºC; R_f: 0.56 (benzene and acetonitrile); λ_{max}: 214.20; IR (KBr, ν_{max}, cm^{-1}): 3270.30 (-NH_2), 3107.72 (C-H), 1687.21 (C=N), 1687.21, 1410.52 (C=C), 1516.06, 1333.65 (-NO_2),

6-[5-[(3-Chlorophenyl)]-4,5-dihydro-1*H*-pyrazol-3-yl]pyrrolo[2,1-*f*][1,2,4]triazin-4-amine (R12): Yield: 32%; colour: brown; m.w.: 294.35; m.p.: 198-200 ºC; R_f: 0.75 (benzene and acetonitrile); λ_{max}: 296.40; IR (KBr, ν_{max}, cm^{-1}): 3201.85 (-NH_2), 3013.59 (C-H), 1665.82 (C=N), 1610.19, 1481.83 (C=C), 544.81 (-Cl),

6-[5-[(4-Fluorophenyl)]-4,5-dihydro-1*H*-pyrazol-3-yl]-pyrrolo[2,1-*f*][1,2,4]triazin-4-amine (R13): Yield: 92%; colour: grey; m.w.: 340.38; m.p.: 192-194 ºC; R_f: 0.58 (benzene and acetonitrile);λ_{max}: 299.40; IR (KBr, ν_{max}, cm^{-1}): 3206.12 (-NH_2), 3052.09 (C-H), 1697.19 (C=N), 1598.78, 1406.24 (C=C), 1216.56 (-F); ^{1}H NMR (500 MHz, $CDCl_3$) δ ppm: 9.93 (NH) 7.207.33 (m, ArH), 3.34 (NH_2), 2.73 (CH_2); ^{13}C NMR (500 MHz, $CDCl_3$) δ ppm: 76.01, 77.06, 77.29, 117.40, 117.28, 119.76, 120.79, 125.70, 129.95, 131.16, 132.57, 133.68, 134.44, 135.49, 137.74, 148.68, 157.76, 160.55, 169.72; MS (*m/z*); Calcd. for $C_{15}H_{11}FN_6$ (296.3023); Found: 297.1531.

6-[5-[(2-Chlorophenyl)]-4,5-dihydro-1*H*-pyrazol-3-yl]-pyrrolo[2,1-*f*][1,2,4]triazin-4-amine (R14): Yield: 89%; colour: brownish; m.w.: 548.12; m.p.: 204-208 ºC; R_f: 0.62 (benzene and acetonitrile); λ_{max}: 306.60; IR (KBr, ν_{max}, cm^{-1}): 3350.17 (-NH_2), 3005.03 (C-H), 1657.26 (C=N), 1601.64, 1430.49 (C=C), 636.09 (-Cl); ^{1}H NMR (500 MHz, ($CDCl_3$) δ ppm: 8.09 (NH), 7.45-7.49 (m, Ar-H), 7.71 (NH_2), 3.12 (CH_2); ^{13}C NMR (500 MHz, ($CDCl_3$) δ ppm: 77.33, 126.02, MS (*m/z*); Calcd. for $C_{15}H_{15}ClN_6$ (330.770); Found: 332.1671.

6-[5-[(2-Bromophenyl)]-4,5-dihydro-1*H*-pyrazol-3-yl]-pyrrolo[2,1-*f*][1,2,4]triazin-4-amine (R15): Yield: 87%; colour: yellow; m.w.: 294.35; m.p.: 172-174 ºC; R_f: 0.55 (benzene and acetonitrile); λ_{max}: 307.20; IR (KBr, ν_{max}, cm^{-1}): 3197.57 (-NH_2), 2999.32 (C-H), 1658.68 (C=N), 1603.06, 1429.06 (C=C), 513.44 (-Br); ^{1}H NMR (500 MHz, $CDCl_3$) δ ppm: 8.48 (NH), 7.03-7.33 (m, Ar-H), 6.94 (NH_2), 3.85 (CH_2); ^{13}C NMR (500 MHz, $CDCl_3$) δ ppm: 45.76, 76., 77.29, 116.68, 120.81, 126.83, 129.70, 130.80, 132.91, 133.05, 134.49, 148.73, 157.37, 169.90. MS (*m/z*) Calcd. for $C_{15}H_{15}BrN_6$ (357.2079); Found: 359.1435.

***In silico* molecular docking study:** In this study, the molecular docking was performed on the crystal structure of the target macromolecule involved in anticancer activity (PDB ID: 8DUG), along with selected synthesized derivatives and a reference standard drug. The crystal structure of PDB ID 8DUG, determined by X-ray diffraction at a resolution of 2.2 Å, represents a key target for investigating ligand binding in estrogen receptor-positive (ER-positive) breast cancer [20].

Absorption, distribution, metabolism and excretion and toxicity (ADMET) prediction: Using Lipinski's rule of 5, the synthesized derivatives and the standard drug were further examined for drug-likeness characteristics. The acceptability of a selected derivative must be evaluated during the drug development. To predict the pharmacokinetic profile (ADME) and toxicity of the ligands, online tools such as SwissADME (http://www.swissadme.ch) [21] and pkCSM (http://biosig.unimelb.edu.au/pkcsm/prediction) [22] were employed, providing *in silico* assessments of small molecule pharmacokinetics and safety.

Anticancer activity: The anticancer screening was carried out in Biocyte Institute of Research and Development Pvt. Ltd., Sangli, India. The National Centre for Cell Science (NCCS), Pune, provided the human mammary gland breast adenocarcinoma (MCF-7) cell line, which was cultured in MEM medium with 10% fetal bovine serum added. Cells were cultured for

24 h at 37 ºC with 5% CO_2 atmosphere and seeded in 100 µL of culture medium at a density of 7×10^4 cells/mL. Test samples (10-100 µg/mL) were then added to the microplates for treatment. The cell line and DMSO (0.2% in PBS) were incubated in control wells. Every sample was incubated three times. To ascertain the proportion of live cells following culture and the survival rate of control cells, controls were kept. In a CO_2 incubator, all cultures were cultured for 24 h at 37 ºC and 5% CO_2. Then 20 µL of MTT reagent (5 mg/mL PBS) was added after the medium had been fully withdrawn. Cells were incubated for 4 h at 37 ºC in a CO_2 incubator following the injection of MTT. The yellowish MTT was reduced to dark coloured formazan by viable cells only when observed under microscope. After removing the medium completely, 200 µL of DMSO was incubated at 37 ºC for 10 min. Triplicate samples were analyzed by measuring the absorbance of each sample by an ELISA microplate reader (BenespheraE21) at a wavelength of 570 nm.

RESULTS AND DISCUSSION

A series of pyrrolotriazine-containing ^{1}H-pyrazole derivatives (**R1-R15**) was synthesized using multi-step reactions as illustrated in **Scheme-I**. In brief, pyrrolotriazine was synthesized *via* the condensation of pyrrole-2-carbaldehyde with hydroxylamine hydrochloride in the presence of a suitable base to afford the corresponding pyrrole oxime intermediate. This intermediate was subsequently acetylated by treatment with acetyl chloride to yield acetyl pyrrolotriazine. In next step, acetyl pyrrolotriazine was then subjected to Claisen-Schmidt condensation with various substituted benzaldehydes under basic conditions to form pyrrolotriazine containing chalcones. Finally, these substituted chalcones were reacted with hydrazine hydrate *via* cyclization to produce the targeted pyrrolotriazine-containing ^{1}H-pyrazole derivatives (**R1-R15**). The structures of the synthesized were confirmed by FT-IR, ^{1}H NMR, ^{13}C NMR and mass spectroscopic analyses.

The IR spectra of all derivatives exhibited characteristic absorption bands corresponding to key functional groups such as -NH_2, -OH, -NO_2, C=N, C=C and C–H, confirming the successful incorporation of these moieties into the pyrrolotriazine-pyrazole framework. The presence of strong stretching vibrations in the 1700–1600 cm^{-1} region was indicative of C=N bonds, while broad peaks around 3400-3200 cm^{-1} confirmed the N–H and O–H functionalities. Substituent-specific signals such as C-F and C-NO_2 were also observed in their characteristic regions, validating the diversity of functionalized derivatives. The ^{1}H NMR spectra of the compounds showed characteristic singlet signals attributed to NH protons of the pyrazole ring, confirming ring closure. Resonances corresponding to aromatic protons appeared in the expected δ 6.8-8.3 ppm range, while aliphatic -CH_2 groups resonated between δ 2.0-3.8 ppm. The ^{13}C NMR spectra further supported these findings, showing signals for C=N (148-165 ppm), C–N and aromatic carbons in the typical chemical shift regions, consistent with the proposed heterocyclic skeleton. Mass spectral of the derivatives displayed molecular ion peaks ($[M + 1]^+$ or $[M + 2]^+$) corresponding to their calculated molecular weights, confirming the molecular composition of the synthesized compounds. The fragmentation patterns observed were consistent with the presence of pyrrolotriazine and pyrazole cores, along with substituent-specific fragments. Collectively, the IR, NMR and mass spectral data confirmed the successful synthesis and structural integrity of the pyrrolotriazine-containing ^{1}H-pyrazole derivatives (**R1-R15**), supporting their suitability for further biological evaluation.

ADMET properties and molecular docking: The physicochemical properties are necessary for the design of new compounds that are intended to use as drugs. A drug-likeness profile can be evaluated *via* parameters of the molecule such as molecular weight (MW), Log p, hydrogen bond acceptors (HBA), hydrogen bond donors (HBD), rotatable bonds, Topological polar surface areas (TPSA), Aqueous solubility and Human intestinal absorption [23]. These parameters were

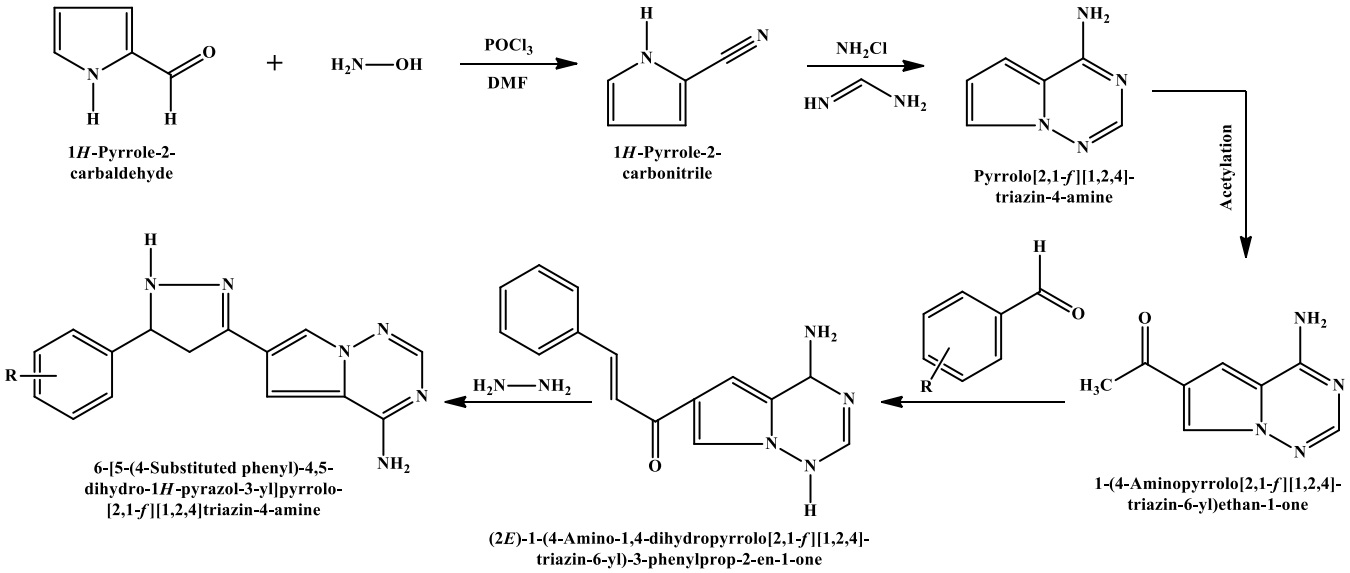

Scheme-I: Synthesis of pyrrolotriazine containing 1*H*-pyrazole compounds (**R1-R15**)

calculated for the synthesized compounds **R1-15** and the results are shown in Table-1.

Lipinski's criteria (MW < 500; HBA ≤ 10 and HBD ≤ 5, rotatable bonds ≤ 10 and TPSA ≤ 140) were used to compute the drug-likeness profiles. It passed the Lipinski rule of five with an acceptable probability score of 85%. A score of 85% was obtained by all compounds **R1-15**, indicating that they had good bioavailability and complied with all five requirements. In order to measure the molecular structure's complexity, the compounds' synthetic accessibility was also evaluated. According to the results (Table-2), which demonstrated that all the compounds lack a complicated synthesis pathway.

In addition to the bioavailability of drugs, metabolism parameters are necessary to recognize whether a molecule has an inhibition activity against certain proteins or not. Compounds **R1-R15** were evaluated for their pharmacokinetic properties, revealing that all derivatives, except compound R_2, were predicted to be non-substrates of P-glycoprotein (P-gp). Since P-gp plays a crucial role in mediating active efflux across pharmacological membranes, this finding suggests favourable cellular permeability [24]. Moreover, all compounds exhibited high gastrointestinal (GI) absorption and were predicted to lack blood-brain barrier (BBB) permeability, indicating a reduced likelihood of central nervous system toxicity. These results, summarized in Table-3, highlight the desirable ADMET characteristics of the synthesized derivatives.

The toxicity of the synthesized compounds **R1-15** was calculated using pkCSM (online software). Compounds **R13** and **R14** were predicted to be non-mutagenic, while the mutagenicity profiles of the remaining derivatives are presented in Table-2.

Molecular docking: Discovery studio 2020 software program was utilized to evaluate the synthesized compounds **R1-15** and 5-fluorouracil for docking investigation. In present

TABLE-1
ADMET PROPERTIES OF SYNTHESIZED COMPOUNDS (**R1-15**) AND STANDARD DRUGS (5-FLUOROURACIL)

Code	m.f.	m.w. (g/mol)	Log P	TPSA (Å^2)	HB donor	HB acceptor	Aqueous solubility (Log mol/L)	Human intestinal absorption (%)	Rotatable bond
R1	$C_{15}H_{16}N_6O$	296.33	1.43	101.35	3	4	-3.634	82.613	2
R2	$C_{15}H_{15}N_7O_2$	325.33	0.73	147.17	3	6	-4.315	79.935	3
R3	$C_{15}H_{16}N_6O$	296.33	1.38	101.35	3	5	-3.532	82.797	2
R4	$C_{15}H_{15}N_6OCl$	330.77	1.63	101.35	3	4	-4.335	83.911	2
R5	$C_{15}H_{15}N_6Br$	357.20	1.93	96.16	2	3	-4.611	91.668	2
R6	$C_{16}H_{18}N_6O$	310.35	1.87	90.35	2	4	-4.071	70.628	3
R7	$C_{15}H_{16}N_6$	280.33	1.07	81.12	2	3	-3.894	70.063	2
R8	$C_{15}H_{16}N_6O$	296.33	1.24	101.35	3	4	-3.529	82.767	2
R9	$C_{16}H_{18}N_6$	294.35	1.98	81.12	2	3	-4.101	92.781	2
R10	$C_{15}H_{15}N_6Br$	357.20	1.88	81.12	2	3	-4.204	93.699	2
R11	$C_{15}H_{15}N_7O_2$	325.33	1.83	10.58	3	5	-3.732	81.165	3
R12	$C_{15}H_{15}N_6OCl$	330.77	2.10	90.35	2	4	-4.071	70.628	3
R13	$C_{15}H_{11}N_6F$	298.32	1.36	98.19	2	4	-3.315	94.424	3
R14	$C_{15}H_{15}N_6OCl$	330.77	1.96	81.12	2	3	-3.346	95.227	2
R15	$C_{15}H_{15}N_6Br$	357.20	1.39	126.94	2	5	-3.457	93.717	3
5-Fluorouracil	$C_4H_3N_2O_2F$	130.08	0.44	65.72	2	3	-1.555	91.698	0

TABLE-2
In silico TOXICITY EVALUATION OF THE COMPOUNDS (**R1-15**)

Code	Acute oral rat toxicity, LD_{50} (mol/kg)	Oral rat chronic toxicity (Log mg/kg bw/day)	Hepatotoxicity	Skin sensitization	*T. pyriformis* toxicity (Log µg/L)	Minnow toxicity (Log mmol/L)	AMES toxicity
R1	2.772	1.707	NO	NO	0.837	1.884	YES
R2	2.769	2.334	NO	NO	0.510	1.682	YES
R3	2.921	1.700	NO	NO	0.876	2.029	YES
R4	3.077	1.575	NO	NO	0.904	1.352	YES
R5	3.130	1.331	NO	NO	1.120	1.242	YES
R6	3.046	1.388	NO	NO	0.962	1.851	YES
R7	3.068	1.400	YES	NO	1.016	1.899	YES
R8	2.918	1.831	NO	NO	0.889	2.082	YES
R9	3.071	1.390	YES	NO	1.060	1.802	YES
R10	2.972	1.393	YES	NO	1.031	1.584	YES
R11	2.914	1.591	NO	NO	0.766	1.837	YES
R12	3.046	1.388	NO	NO	0.962	1.851	YES
R13	2.750	1.191	YES	NO	0.337	0.968	NO
R14	2.563	1.040	YES	NO	0.337	-1.397	NO
R15	2.465	1.884	NO	NO	0.320	0.956	YES
5-Fluorouracil	1.939	1.587	NO	NO	-0.236	3.152	NO

TABLE-3
DRUG LIKENESS, BIOAVAILABILITY AND SYNTHETIC ACCESSIBILITY SCORE

Code	BBB	PGP substrate	Total clearance (log) mL/min/kg)	Bioavailability score	Maximum tolerated dose (Log mg/kg d)	Synthetic accessibility	Lipinski's rule violations
R1	-0.409	NO	0.129	0.55	-0.267	4.11	YES (0)
R2	-0.662	YES	0.603	0.55	-0.616	4.19	YES (0)
R3	-0.407	NO	0.713	0.55	-0.0439	4.09	YES (0)
R4	-0.591	NO	0.219	0.55	-0.36	4.10	YES (0)
R5	-0.352	NO	0.137	0.55	-0.376	4.09	YES (0)
R6	-0.385	NO	0.809	0.55	-0.644	4.16	YES (0)
R7	-0.157	NO	0.851	0.55	-0.527	4.08	YES (0)
R8	-0.404	NO	0.707	0.55	-0.438	4.09	YES (0)
R9	-0.150	NO	0.862	0.55	-0.592	4.19	YES (0)
R10	-0.172	NO	0.857	0.55	-0.313	4.14	YES (0)
R11	0.609	NO	0.717	0.55	-0.567	4.08	YES (0)
R12	-0.385	NO	0.879	0.55	-0.644	4.07	YES (0)
R13	-0.573	NO	0.528	0.55	-0.297	4.07	YES (0)
R14	-0.787	NO	-0.059	0.55	-0.08	4.09	YES (0)
R15	-0.865	NO	0.465	0.55	-0.247	4.13	YES (0)
5-Fluorouracil	-0.388	NO	0.639	0.55	1.359	4.07	YES (0)

work, the designated protein model was the crystal structure domain in complex with 5-fluorouracil (PDB ID 8DUG) with 2.20 resolution. The program default was defined the legends rotatable bonds. In comparison with 5-fluorouracil (as reference), the highest score of the ligands (**R1**-**R15**) docking results are listed in Table-4. Docking score results were ranged from -8.3 Kcal/mol to -10.5 Kcal/mol against (8DUG) active side. The selected amino acids for the enzyme active site were (HIS553, HIS377, ASN519, ASP465, GLY516, ALA701, GLY518, TYR552, PHE209, ARG210). The 5-fluorouracil docking result score was (-5.2 Kcal/mol). The results showed that the interactions took place between the receptor in the

TABLE-4
BINDING AFFINITY, H BOND AND VAN DER WAALS INTERACTION OF DESIGNED DERIVATIVES ON PROTEINS 8DUG

Derivatives	Binding affinity (docking) (Kcal/mol)	H bond	van der Waals interaction
R1	-9.0	GLU424, ASP387, ASP453	LYS699, ASN257, LEU428, GLY427, PHE426, GLU425, HIS553, TYR549, SER454, ASN519, ARG210, TYR700, PHE209
R2	-10.5	GLU425, GLU424, ASP387, ASP453, ARG534, ASN698, TYR700	HIS553, HIS377, ASN519, ASP465, GLY516, ALA701, GLY518, TYR552, PHE209, ARG210
R3	-9.8	ASP387, ASP453, ASN257, GLU424	ILE456, TYR549, GLU457, ASN519, HIS553, TYR700, GLY518, PHE209, LYS699, LEU428, GLY427
R4	-9.8	ALA232, PHE235	ASP233, PRO237, PRO231, ALA236, GLY548, PRO550, TYR549, GLU457, TYR566, GLY458, ASN549, SER547
R5	-8.8	GLN254, VAL208	TYR549, TYR552, TYR234, GLY548, SER547, ASN698, ARG463, ARG534, GLY518, LYS207, PHE209
R6	-8.9	ASP387, ASP553, TYR552, GLY206	HIS553, GLU425, SER547, TYR700, LYS207, PHE209, TYR234, GLY548, ARG536, ASN519
R7	-9.7	ASP714, ASN216, THR182	LYS718, PHE713, PHE186, PHE185, LEU219, HIS697, LYS215, SER696
R8	-8.5	GLN254, VAL208	TYR549, TYR552, TYR234, GLY548, SER547, ASN698, ARG463, ARG534, GLY518, LYS207, PHE209
R9	-8.6	ILE456	ILE386, GLU457, TYR549, GLY548, SER547, LYS207, GLY206, VAL208, PHE209, TYR234
R10	-8.5	ALA232, PHE235	ASP233, PRO237, PRO231, ALA236, GLY548, PRO550, TYR549, GLU457, TYR566, GLY458, ASN549, SER547
R11	-9.9	GLN254, ASN519, VAL208	TYR234, GLY548, TYR552, SER547, GLY518, ARG534, SER517, ARG536, ASN698, LYS213, PHE209
R12	-8.3	GLU457	ILE456, SER454, TYR549, ASP387, LYS207, VAL208, GLY206, GLN256, TYR236, TYR552, ARG536
R13	-10.3	TYR700, LYS699	SER454, ASP387, TYR552, HIS553, GLY518, PHE209, GLY427, ASN519, ARG536, GLU457
R14	-10.0	GLN254, SER547, VAL208	TYR234, ARG210, TYR552, GLY206, LYS207, LYS213, PHE209, ARG210, TYR205,
R15	-9.7	ASP714, ASN216, THR182	LYS718, PHE713, PHE186, PHE185, LEU219, HIS697, LYS215, SER696
5-Fluorouracil	-5.2	ASP351	LEU549, THR347, LEJ354, GLU353, ARG334, LEU384, MET528

pocket with 5-fluorouracil and just 4 ligands (Fig. 1). Also, the results indicated that the top docking score was for compound **R2** (-10.5 Kcal/mol). The interactions of bond lengths and hydrogen bonds in site were performed and the results are displayed in Table-4. As shown in Table-4, 5-fluorouracil formed H-π interactions with amino acid residues, while

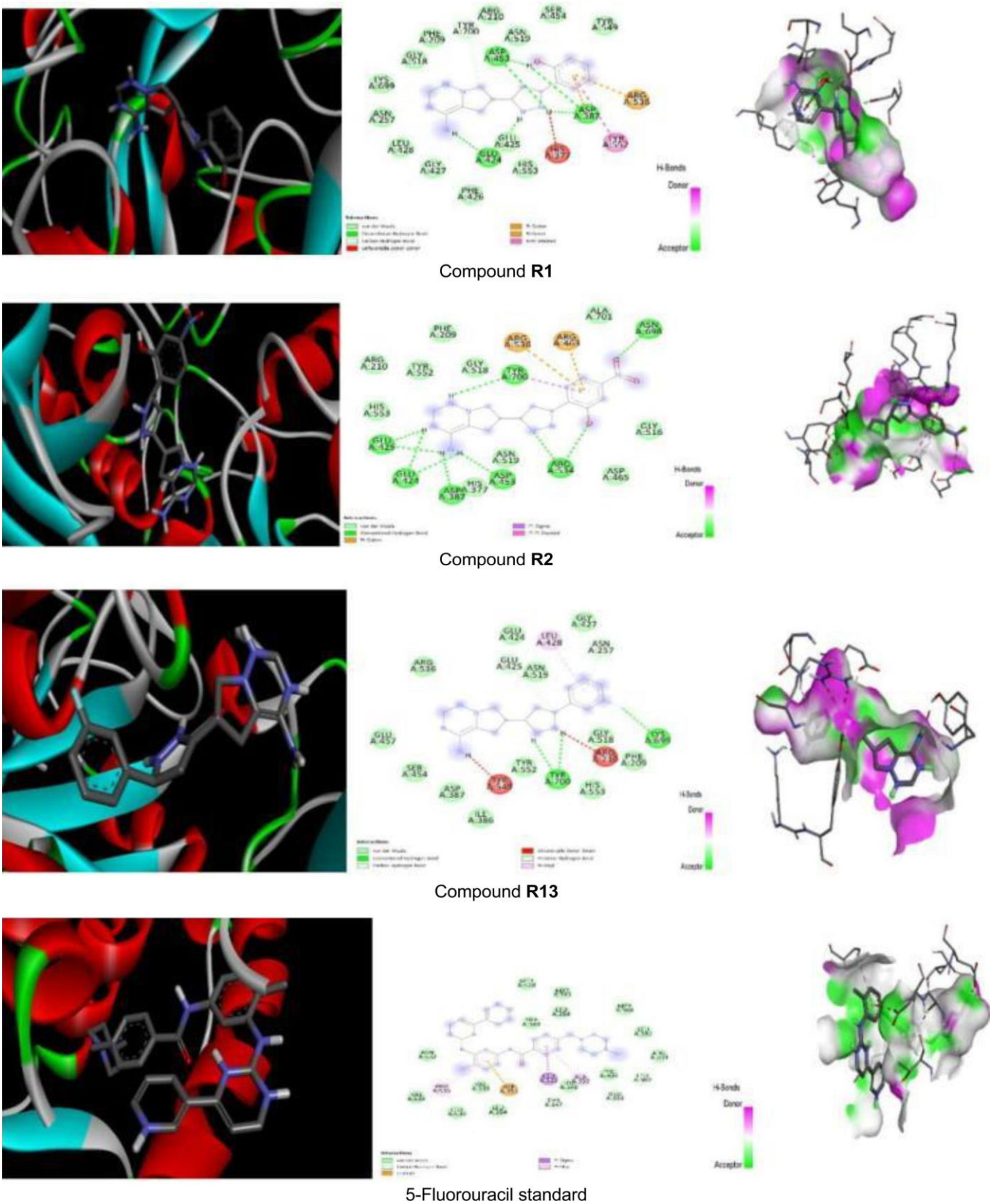

Fig. 1. Ligand-receptor interaction along with the bond length and amino acid residues and hydrogen bond interaction against 8DUG

TABLE-5
EFFECT OF SAMPLE BY MTT ASSAY AGAINST MCF-7 CELL LINE

Code	Concentration (µg/mL)	Absorbance				Cell viability	IC_{50}
		1	2	3	Average		
C	Control	2.107	2.114	2.110	2.110	–	–
R1	10	1.327	1.325	1.326	1.315	62.79	40.21
	40	0.956	0.955	0.952	0.954	45.22	
	100	0.745	0.746	0.741	0.744	35.26	
R2	10	1.253	1.256	1.254	1.254	59.44	37.94
	40	0.974	0.976	0.926	0.975	46.22	
	100	0.732	0.736	0.738	0.735	34.84	
R13	10	1.354	1.356	1.359	1.356	64.28	42.75
	40	0.941	0.942	0.946	0.944	44.69	
	100	0.721	0.72	0.725	0.772	34.21	
5-Fluorouracil	10	0.512	0.513	0.515	0.513	24.32	6
	40	0.400	0.412	0.416	0.412	16.55	
	100	0.306	0.307	0.303	0.305	14.46	

hydrogen bond acceptor interactions were observed between 5-fluorouracil and both amino acids as well as surrounding water molecules.

Anticancer activity: The MTT (3-[4,5-dimethylthiazol-2-yl]-2,5-diphenyltetrazolium bromide) assay was used to assess the synthetic compounds' *in vitro* anticancer activity against the MCF-7 with 5-fluorouracil (5-FU) acting as the standard reference drug. Among the synthesized series, compounds **R1**, **R2** and **R13** displayed significant cytotoxic activity, with IC_{50} values, indicating their efficacy as effective anticancer agents as shown in Table-5. These findings recommend that the active compounds may induce cell death by interfering with cellular metabolic pathways or DNA synthesis, thus highlighting their promise for further development in breast cancer chemotherapy.

Conclusion

In this study, a series of 15 pyrrolotriazine-containing ^{1}H pyrazole derivatives (**R1-R15**) were successfully synthesized *via* multi-step reactions and thoroughly characterized by FT-IR, ^{1}H NMR, ^{13}C NMR and mass spectrometry, confirming the successful synthesis of the target molecules. The ADMET and drug-likeness analyses indicated that these derivatives possess favourable pharmaco-kinetic properties, including high gastrointestinal absorption, low blood-brain barrier permeability and minimal P-glyco-protein interaction, suggesting good oral bioavailability and reduced systemic toxicity. The molecular docking studies against the crystal structure of the anticancer target protein (PDB ID: 8DUG) demonstrated strong binding affinities of the synthesized compounds, with several ligands outperforming reference drug 5-fluorouracil, highlighting their potential as effective inhibitors. Notably, compounds **R1**, **R2** and **R13** showed the most promising *in vitro* anticancer activity against MCF-7 breast cancer cells, indicating their ability to interfere with key cellular pathways and induce cytotoxic effects. These findings establish pyrrolotriazine-containing ^{1}H-pyrazole derivatives as a promising scaffold for the development of novel anticancer agents, necessitating further potential as therapeutic candidates against breast cancer.

ACKNOWLEDGEMENTS

The authors are thankful to the Kamla Nehru College of Pharmacy, Butibori, Nagpur for providing facilities to carry out the research work. The authors are also thankful to Director, SAIF, Panjab University, Chandigarh for providing Spectral Data and thankful to Dr. Sandeep Patil, Director, Biocyte Institute of Research and Development, Sangli for anticancer activities.

CONFLICT OF INTEREST

The authors declare that there is no conflict of interests regarding the publication of this article.

REFERENCES

1. R.J. Obaida, N. Naeem, E.U. Mughal, M.M. Al-Rooqi, A. Sadiq, R.S. Jassas, Z. Moussa and S.A. Ahmed, *RSC Adv.*, **12**, 19764 (2022); https://doi.org/10.1039/D2RA03081K
2. D. Havrylyuk, O. Roman and R. Lesyk, *Eur. J. Med. Chem.*, **113**, 4145 (2016); https://doi.org/10.1016/j.ejmech.2016.02.030
3. F.T. Biswas, R.K. Mittal, V. Sharma, Kanupriya and I. Mishra, *Med. Chem.*, **20**, 369 (2024); https://doi.org/10.2174/0115734064278334231211054053
4. A.A. Abbas, T.A. Farghaly and K.M. Dawood, *RSC Adv.*, **14**, 19752 (2024); https://doi.org/10.1039/D4RA01387E
5. D. Kumar and S.K. Jain, *Curr. Med. Chem.*, **23**, 4338 (2016); https://doi.org/10.2174/0929867323666160809093930
6. M.H.A. Al-Jumaili, E.A. Bakr, M.A. Huessien, A.S. Hamed and M. J. Muhaidi, *Heterocycl. Commun.*, **31**, 20220179 (2025); https://doi.org/10.1515/hc-2022-0179
7. A. Omar, *Al-Azhar J. Pharm. Sci.*, **62**, 39 (2020); https://doi.org/10.21608/ajps.2020.118375
8. T.H. Iorkula, O.J.-K. Osayawea, D.A. Odogwu, L.O. Ganiyu, E. Faderin, R.F. Awoyemi, B.O. Akodu, I.H. Ifijen, O.R. Aworindee, P. Agyemang and O.L. Onyinyechi, *RSC Adv.*, **15**, 3756 (2025); https://doi.org/10.1039/D4RA07556K
9. T.T. Yadav, G.M. Shaikh, M.S. Kumar, M. Chintamaneni and Y.C. Mayur, *Front Chem.*, **10**, 861288 (2022); https://doi.org/10.3389/fchem.2022.861288
10. V. Sharma, R. Kamal and V. Kumar, *Curr. Top. Med. Chem.*, **17**, 2482 (2017); https://doi.org/10.2174/1568026617666170307113744

11. J.S. Brown, S.R. Amend, R.H. Austin, R.A. Gatenby, E.U. Hammarlund and K.J. Pienta, *Mol. Cancer Res.*, **21**, 1142 (2023); https://doi.org/10.1158/1541-7786.MCR-23-0411
12. J. Yayan, K.-J. Franke, M. Berger, W. Windisch and K. Rasche, *Mol. Biol. Rep.*, **51**, 165 (2024); https://doi.org/10.1007/s11033-023-08920-5
13. J. Ferlay, M. Colombet, I. Soerjomataram, C. Mathers, D.M. Parkin, M. Piñeros, A. Znaor and F. Bray, *Int. J. Cancer*, **144**, 1941 (2019); https://doi.org/10.1002/ijc.31937
14. W. Liu, J. Fang, M. Zhu, J. Zhou and C. Yuan, *BMC Pediatr.*, **25**, 571 (2025); https://doi.org/10.1186/s12887-025-05847-7
15. R.L. Siegel, A.N. Giaquinto and A. Jemal, *CA Cancer J. Clin.*, **74**, 12 (2024); https://doi.org/10.3322/caac.21820
16. S. Yu, Y. Wang, P. He, B. Shao, F. Liu, Z. Xiang, T. Yang, Y. Zeng, T. He, J. Ma, X. Wang and L. Liu, *Front Oncol.*, **12**, 809304 (2022); https://doi.org/10.3389/fonc.2022.809304
17. B. Liu, H. Zhou, L. Tan, K.T.H. Siu and X.-Y. Guan, *Sig. Transduct. Target Ther.*, **9**, 175 (2024); https://doi.org/10.1038/s41392-024-01856-7
18. M.F. Mercogliano, S. Bruni, F.L. Mauro and R. Schillaci, *Cancers*, **15**, 1987 (2023); https://doi.org/10.3390/cancers15071987
19. Z. Bernat, A. Szymanowska, M. Kciuk, K. Kotwica-Mojzych and M. Mojzych, *Molecules*, **25**, 3948 (2020); https://doi.org/10.3390/molecules25173948
20. G.R. Hancock, K.S. Young, D.J. Hosfield, C. Joiner, E.A. Sullivan, Y. Yildiz, M. Lainé, G.L. Greene and S.W. Fanning, *npj Breast Cancer*, **8**, 130 (2022); https://doi.org/10.1038/s41523-022-00497-9
21. A. Daina, O. Michielin, and V. Zoete, *Sci. Rep.*, **7**, 42717 (2017); https://doi.org/10.1038/srep42717
22. D.E.V. Pires, T.L. Blundell, and D.B. Ascher, *J. Med. Chem.*, **58**, 4066 (2015); https://doi.org/10.1021/acs.jmedchem.5b00104
23. C.A. Lipinski, F. Lombardo, B.W. Dominy and P.J. Feeney, *Adv. Drug Delivery Rev.*, **23**, 3 (1997); https://doi.org/10.1016/S0169-409X(96)00423-1
24. N. Guéniche, A. Huguet, A. Bruyere, D. Habauzit, L. Le Hégarat and O. Fardel, *Biopharm. Drug Dispos.*, **42**, 393 (2021); https://doi.org/10.1002/bdd.2299